Influence of ply-drop position in thickness direction on static and fatigue loading behaviour of carbon fibre epoxy laminates

Ambrosius Weiss, Laurent Michel, Stephane Mahdi, Estelle Cross, Jean-Jacques Barrau

Influence of ply-drop position in thickness direction on static and fatigue loading behaviour of carbon fibre epoxy laminates

A. Weiss[1], L. Michel[1], S. Mahdi[2], E. Cros[2], J.J. Barrau[3]
1 : Université de Toulouse ; INSA,UPS, Mines Albi, ISAE
ICA (Institut Clément Ader), DMSM
, ISAE – F – 31055 Toulouse
e-mail : aweiss@isae.fr, lmichel@isae.fr

2 : Airbus France – Toulouse
e-mail : stephane.mahdi@airbus.com, estelle.cros@airbus.com

3 : Université de Toulouse ; INSA,UPS, Mines Albi, ISAE
ICA (Institut Clément Ader), LGMT
Université de Toulouse – F - 31062 Toulouse
e-mail : barrau@cict.fr

SUMMARY

The influence of ply-drop position in thickness direction under fatigue loading (R = -1) has been studied. Two configurations with different ply-drop positions which drop from 20 to 12 plies have been compared. Fatigue tests and finite element simulations were performed to identify the damage modes, spots and kinetics before final failure.

Keywords: ply-drop, fatigue, damage modes, numerical simulation, composite

INTRODUCTION

Recent developments in structural design show an increasing application of laminated composite materials in complex structures. To match structural requirements, the thickness of structural parts has to vary depending on the introduced loads. These thickness variations are realised by so called ply drop-offs. In these zones the state of stress changes and stress concentrations are expected. Studies about damage modes and propagation in these zones caused by stress concentrations have already been carried out [1,3,4,6]. For a simple specimen geometry some design guidelines have been proposed to avoid or minimise damage [2,5]. These basic studies give an idea about the influence of ply-drops on the static and fatigue load behaviour. The present study goes further in terms of mechanical behaviour of a specimen with several ply-drops. The objective of the study is to evaluate the influence of ply-drop position on structural resistance on static and fatigue loading and finally on the *SN* curve. To do so two ply-drop configurations representative of industrial applications with different ply-drop positions have been tested. Damage spots as well as the damage kinetics before final failure were observed during fatigue mechanical tests. The observed phenomena and kinetics contributes to explain the differences in fatigue lifetime of the two tested configurations. Some phenomena observed experimentally are also analysed with the help of the interlaminar stress state calculated with a finite element model.

SPECIMEN SETUP AND CONTROL DURING TEST

Testing material and specimens' dimensions

The used material is a pre-impregnated carbon fibre/epoxy composite delivered by Hexcel (T700-M21 268 g), the thickness of the UD plies is 0.25 mm. The ply-drop zone is non symmetrical with an angle of 7°.

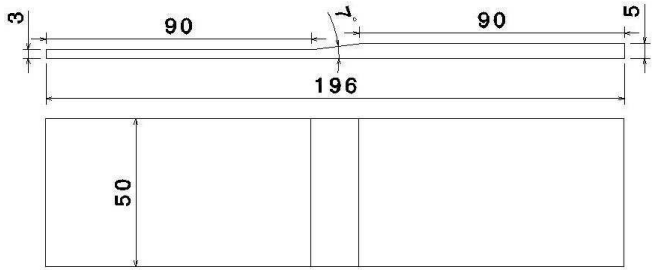

Figure 1: Geometry of ply-drop specimen

Stacking sequence

Test specimen drop from 20 to 12 plies by respecting the usual guidelines for ply-drop zones. The base laminates of the thick and the thin section are strongly orientated with 50% of the plies at 0°. These base laminates and the dropped plies are the same for the two tested configurations. As the first two ply-drops close to the thin section are considered the most critical for damage initiation, the position of these ply-drops has been varied. To vary this position the order of ply-drops has been permuted which leads to a configuration with ply-drops 1and 2 close to the mid plane (V_{int}) and another one with ply-drops 1 and 2 far from the mid plane (V_{ext}) as shown in Figure 2.

V_{int}

20	90	90	90	90	90	90	90	90	90
19	45	45	45	45	45	45	45	45	45
18	0	0							
17	0	0	0	0	0	0	0	0	0
16	-45	-45	-45	-45	-45	-45			
15	0	0	0	0	0	0	0	0	0
14	45	45	45	45					
13	0	0	0	0	0	0	0	0	
12	-45	-45	-45	-45	-45	-45	-45	-45	-45
11	0	0	0	0	0	0	0	0	0
10	0	0	0	0	0	0	0	0	0
9	-45	-45	-45	-45	-45	-45	-45	-45	-45
8	0	0	0	0	0	0	0		
7	45	45	45						
6	0	0	0	0	0	0	0	0	0
5	-45	-45	-45	-45	-45				
4	0	0	0	0	0	0	0	0	0
3	0								
2	45	45	45	45	45	45	45	45	45
1	90	90	90	90	90	90	90	90	90
No.	**8**	**7**	**6**	**5**	**4**	**3**	**2**	**1**	

V_{ext}

20	90	90	90	90	90	90	90	90	90
19	45	45	45	45	45	45	45	45	45
18	0	0	0	0	0	0	0	0	
17	0	0	0	0	0	0	0	0	0
16	-45	-45	-45	-45					
15	0	0	0	0	0	0	0	0	0
14	45	45	45	45	45	45			
13	0	0							
12	-45	-45	-45	-45	-45	-45	-45	-45	-45
11	0	0	0	0	0	0	0	0	0
10	0	0	0	0	0	0	0	0	0
9	-45	-45	-45	-45	-45	-45	-45	-45	-45
8	0								
7	45	45	45	45	45				
6	0	0	0	0	0	0	0	0	0
5	-45	-45	-45						
4	0	0	0	0	0	0	0	0	0
3	0	0	0	0	0	0	0		
2	45	45	45	45	45	45	45	45	45
1	90	90	90	90	90	90	90	90	90
No.	**8**	**7**	**6**	**5**	**4**	**3**	**2**	**1**	

Figure 2: Stacking sequence for the two tested ply-drop configurations with ply-drops 1 and 2 close the mid plane (V_{int}) and far from the mid plane (V_{ext})

Testing conditions and damage observation

All static and fatigue tests have been carried out on a hydraulic Instron testing machine with a maximal capacity of 300 kN. Under compression load the specimens' non symmetry creates a bending moment which causes a displacement of the specimen perpendicular to the load direction. To avoid this deflection which is not representative of a panel structure under real conditions, the specimens have been clamped in an anti-buckling device (Figure 3). Furthermore this device maintains the specimens' position while tested. Teflon pads have been inserted to minimise friction in the non-clamped zone.

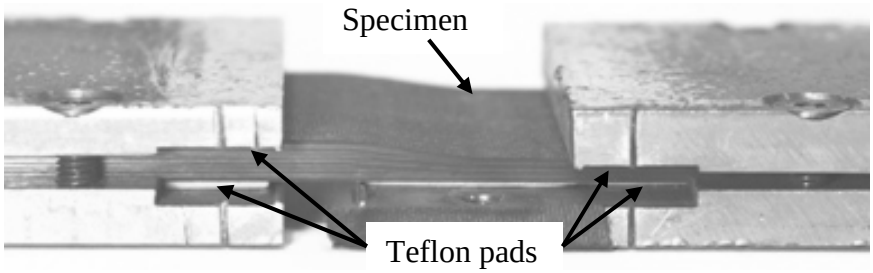

Figure 3: Specimen clamped in the anti-buckling device

To monitor the damages during fatigue loading the tests have been stopped regularly and both sides have been observed with an optical microscope. As the specimen have not been removed from the testing machine when the tests have been stopped it has been possible to apply a static load. This makes easier the detection of crack damages by the optical observation.

Damage kinetics during the last cycles before final failure have been filmed by a camera (60 images/s) on one side of the specimen. The specimen's displacement has also been recorded by an extensometer placed on the anti-buckling device.

FINITE ELEMENT MODELLING

To calculate the state of interlaminar stress a global-local 3D finite element model has been implemented with the code Samcef©. The local model is designed to correctly represent the free-edge effects.

Geometry and boundary conditions of the global-local model

The global model represents the complete ply-drop zone plus the unclamped part of the base laminates in the thick and the thin section including the teflon part of the anti-buckling device. To simulate the conditions of a specimen clamped in the testing machine, on the right side all degrees of freedom are restrained, idem on the left side except for the displacement in load direction. The laminate is modelled ply by ply with 20 nodes cubic elements with one element in the plies' thickness direction. The triangular zones at the ply-drops are modelled by splines to avoid a brutal changing in

the slope. 15 nodes elements and the material data of the matrix material have been used in these triangles. The anti-buckling device is meshed by 15 nodes elements with material data for usual steel. No friction has been considered for modelling the contact between the specimen and the anti-buckling device. The meshing in the specimen's width direction has been optimised in terms of computational time and required precision. Edge effects cause high stress variations close to the specimen's sides therefore the elements close to the borders are cubic. In the specimen's middle stress variations being comparatively smaller; a coarser meshing has been chosen along width direction.

In order to refine the meshing without immoderately increasing computational time, a local model has been developed. This local model represents the zone around a ply-drop with one ply on top and one on bottom of the dropped ply, thus there are as many local models as ply-drops. The displacements of the global model around the zone formed by the local model have been saved. With these global displacements, the displacements for the local models have been interpolated with a local linear Matlab function. To minimise problems with stress singularities the interlaminar stresses has been calculated within interface elements with infinite rigidity which have been inserted between the plies. A mesh refinement study has shown that stress values are correctly represented with one element per ply for the global model and 2 elements per ply for the local model by keeping elements cubic at the specimen edges. All material laws are linear elastic, the solver module is non-linear.

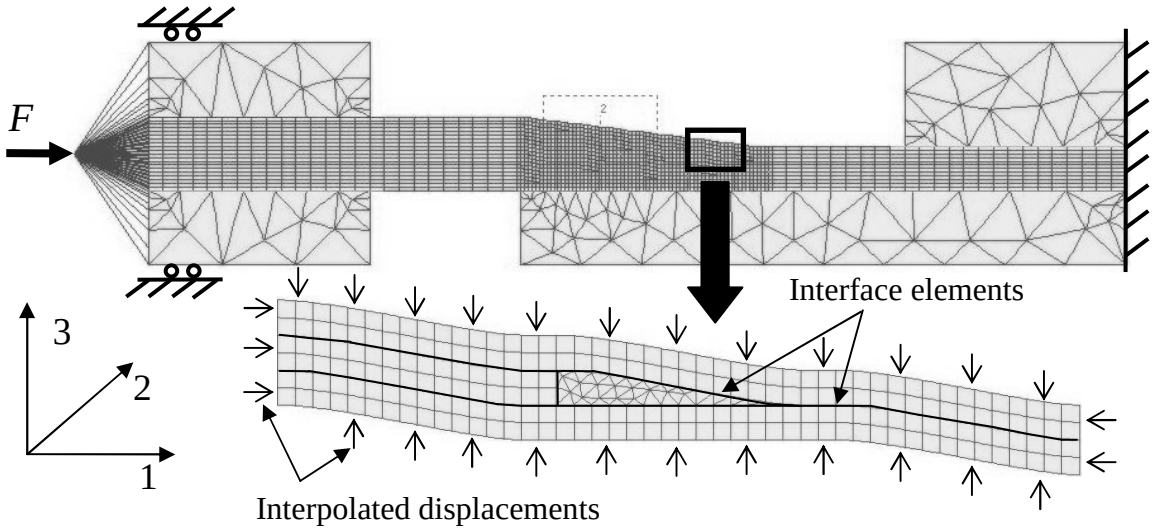

Figure 4: Global-local model of a specimen

Method for calculation of representative values

There are two main problems when calculating numerical stresses around ply-drops, the stress singularity because of the dropped ply and the edge-effect at the free edges. Convergence studies have shown that the average stress values calculated for a squared zone of 0.25 x 0.25 mm already converge for a meshing of 2 elements per ply. The dashed regions in Figure 5 show the zones of the interface elements used for calculating the average stress values. With this method it is possible to quickly and directly compare the stress values on both edges, in the middle and between different ply-drops.

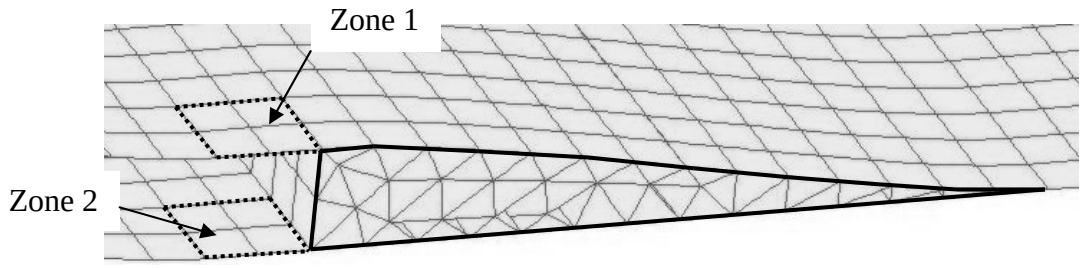

Figure 5: Zones used to averaged the interlaminar stresses at the specimens' edges

RESULTS AND ANALYSIS

Static tests

The static compression tests have been performed with a loading rate of 20 kN/min, and on tension equal to 40 kN/min. Failure stresses in the thin section and the standard deviations are given in Table 1. Four tests on tension/compression have been achieved for the V_{int}, five for the V_{ext}.

Table 1: Static failure stresses (Standard deviation)

Configuration	**V_{int}**	**V_{ext}**
Average stress for compression load (MPa)	-452 (±14)	-473 (±6)
Average stress for tension load (MPa)	819 (±46)	922 (±24)

It is important to notice that the failure stresses under compression and tension load of the V_{int} are lower than the V_{ext}. Furthermore for both configurations the failure stresses on tension load are nearly two times higher than on compression, thus the most critical value is the compression load of the V_{int}.

Fatigue test parameters

The load ratio is R = -1, the frequency has been fixed to 5 Hz. To allow a direct comparison of fatigue lifetime, the load levels are the same for both configurations, they are fixed as a function of the static compression failure stress of the V_{int} (70, 60, 50 and 45%).

Distribution of fatigue damages observed on both specimen sides

By stopping the fatigue tests regularly and observing the two edges of the specimen, the damage modes and spots have been identified. A non-symmetrical distribution of delaminations on the specimen's edges has been found. An example is given in Figure 6 which shows the 2nd ply-drop of the V_{int} and V_{ext}. For both configurations there are delaminations on side 2 but no visible damage on side 1.

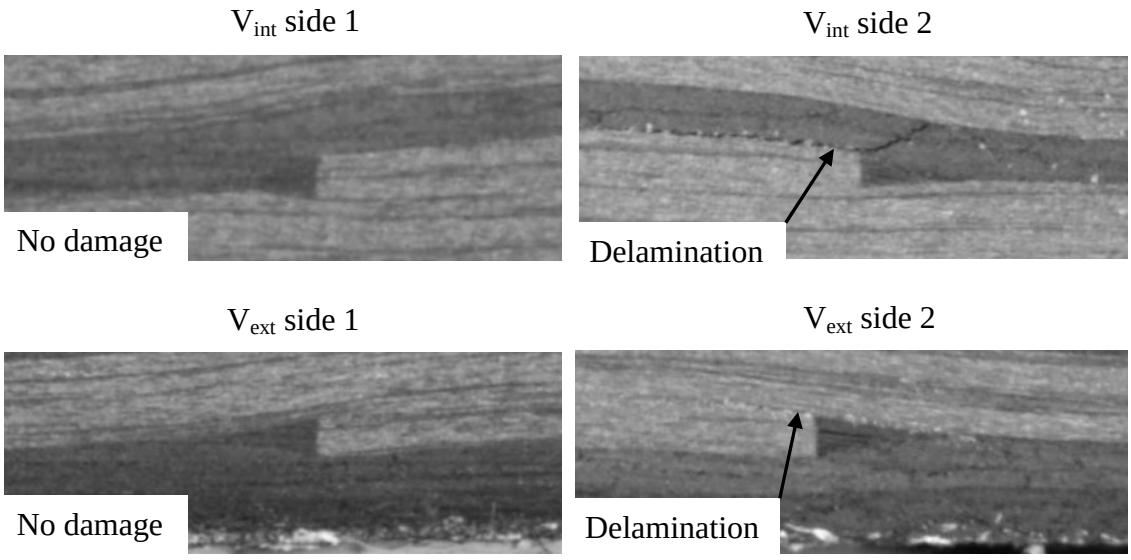

Figure 6: Delamination at 2nd ply-drop of V_{int} (top) and V_{ext} (bottom) tested at 50%, interrupted at 8000 cycles

Table 2 shows the frequency of delaminations identified in fatigue tests and the interlaminar stresses calculated in zone 1 with the global-local model for a compression loading at static failure stress of the V_{int}. The shear stresses in 23 direction are small compared to the other values and have been considered negligible.

Table 2: Frequency of delaminations observed in fatigue tests and calculated interlaminar stresses

	V_{int}		**V_{ext}**	
	Side 1	**Side 2**	**Side 1**	**Side 2**
Observed frequency of delaminations / Total number of tests	1 / 5	4 / 5	0 / 7	7 / 7
Opening 33 (MPa)	44	51	26	15
Shear 13 (MPa)	65	145	131	191

It is important to notice that for the V_{int} delaminations appear preferably on side 2, at this side the opening stress 33 and shear stress 13 are higher than on the other side. The

same for the V_{ext}, the delaminations appear preferably on side 2, there the shear stress 13 is higher but the opening stress 33 is lower than on the other side.

Comparing the test results with the numerical values shows that on the preferred side for delaminations the shear stress 13 is always higher. The opening stress 33 doesn't show this clear tendency but its absolute values are low compared to the shear stress 13.

Critical delamination spots in the ply drop-off zone

Observations during fatigue tests show that for the configuration V_{int} as well as V_{ext} the delaminations initiate around ply-drops 1 and 2.Figure 7 shows side 2 of a specimen V_{int} where delaminations initiated around ply-drop 1 and 2.

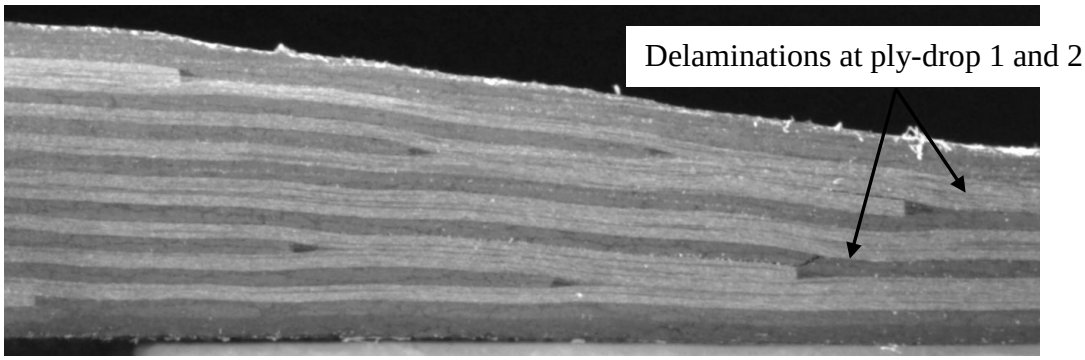

Figure 7: Side 2 of a V_{int} tested at 50% and stopped at 10000cycles with delaminations around ply-drop 1 and 2

Figure 8 and Figure 9 show the interlaminar stresses calculated at ply drop 1 to 4 with the global-local model in zone 1 on both sides and in the middle of the specimen for the V_{int} and the V_{ext}. The experimental observations have been related with the numerical simulations. The experimentally identified critical delamination spots are ply-drop 1 and 2, therefore the calculated stresses at these ply-drops will be compared to the stresses at ply-drop 3 and 4.

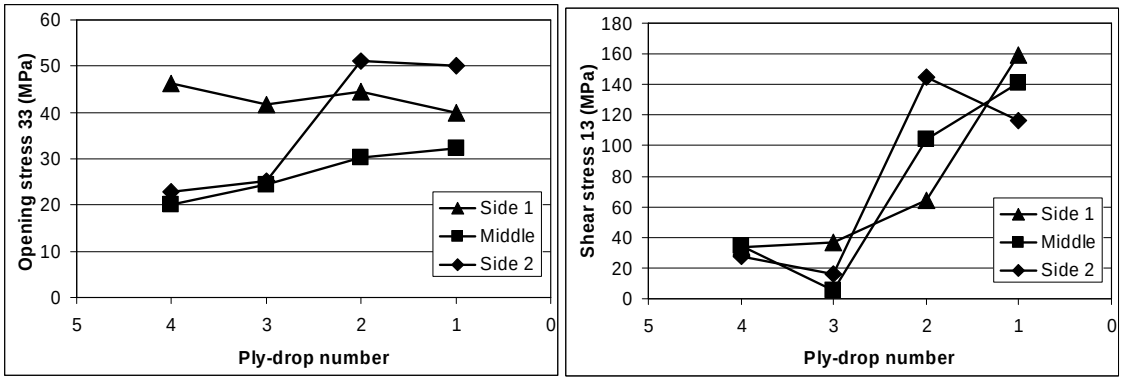

Figure 8: Interlaminar stresses in zone 1 at ply-drop 1 to 4 for the V_{int}

For the V_{int}, at ply-drops 1 and 2 the opening stress 33 is slightly higher but the shear stress 13 is much higher. In general the absolute values of the shear stress 13 are much higher than the opening stress 33.

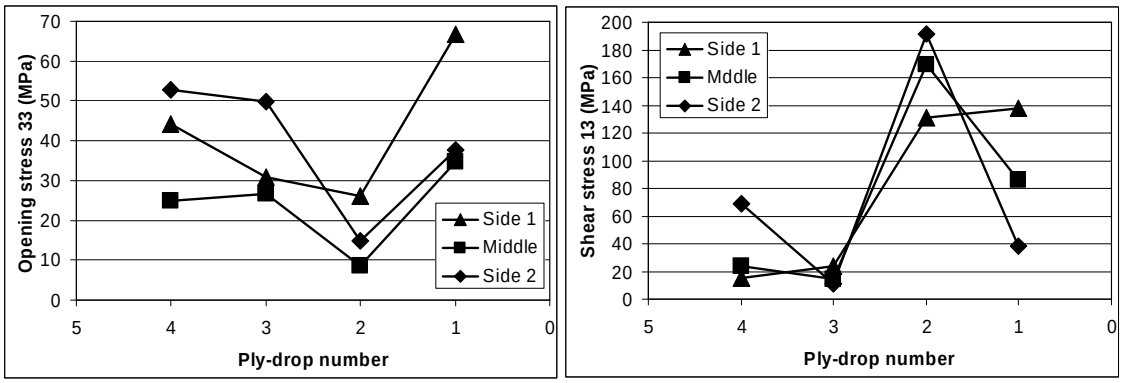

Figure 9: Interlaminar stresses in zone 1 at ply-drop 1 to 4 for the V_{ext}

For the V_{ext} (Figure 9), the opening stress has its highest value at ply-drop 1, but decreases at ply-drop 2 to a value even lower than at ply-drops 3 and 4. The shear stress 13 at ply-drops 1 and 2 is at least on one side higher than at ply-drops 3 and 4. The general level of absolute values of shear stress is much higher than the opening stress 33 as for the V_{int}.

The mechanical tests have shown that for both configurations the critical spots of delamination initiation are the ply-drops 1 and 2. The numerical simulations show that at ply-drops 1 and 2 the interlaminar shear stress 13 is higher than at the other ply-drops with a general high level compared to the other interlaminar stress components. The opening stress 33 presents lower absolute values and doesn't show a clear tendency.

Final failure on fatigue loading

To study the damage kinetics one side of the specimen has been filmed with a camera. The observations show that there are three stages during cyclic loading, cycling without damage, damage initiation with stable propagation and finally unstable propagation until final failure.

The films show that before final failure both configurations are separated in three sub-laminates, resulting from the delamination propagation around ply-drops 1 and 2. Figure 10 sketches the separation of the two configurations.

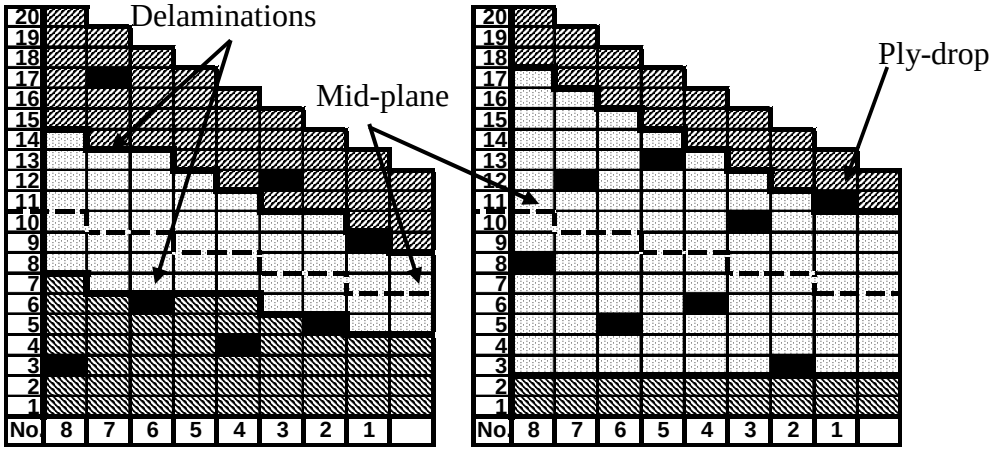

Figure 10: Separation of V_{int} (left) and V_{ext} (right) in three sub-laminates before failure

The V_{int} is separated in three sub-laminates of same size which transfer nearly the same load. During cyclic loading these sub-laminates bend independently until one of them breaks which causes a load-redistribution to the other two sub-laminates and quickly the final failure. The V_{ext} is separated in two small sub-laminates on top and bottom and one big in the middle. This big sub-laminate transfers most of the load; its breakage leads to final failure.

The differences between the two tested configurations in fatigue lifetime are shown with a semi-logarithmical SN curve in Figure 11. The value at N = 1 is the static compression failure stress.

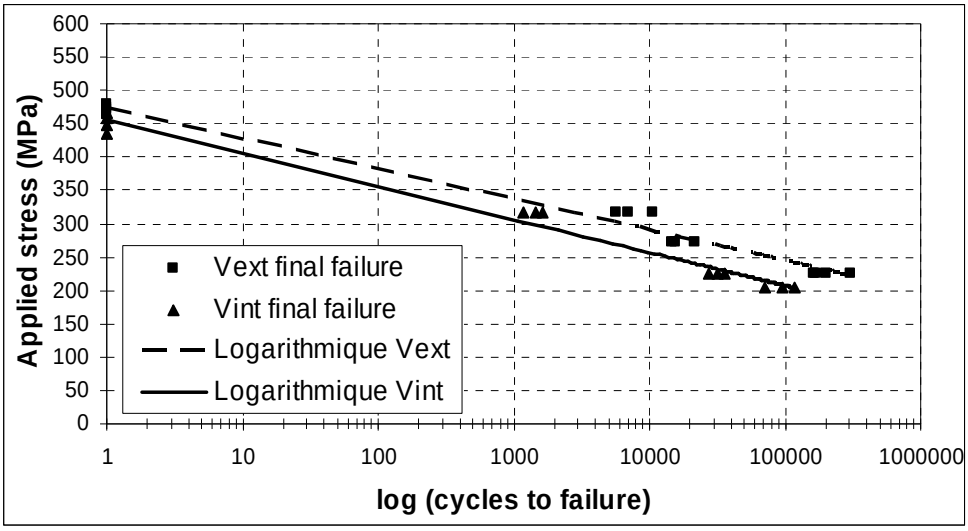

Figure 11: Semi-logarithmical SN curve for the two tested configurations V_{int} and V_{ext}

The two curves are nearly parallel, the slope of the V_{ext} is slightly flatter, but the V_{int} is vertically shifted to lower values. The results show that the vertical position of the ply-drops influences the fatigue lifetime. Contrary to the general guideline to place the ply-drops close to the mid-plane, the tested configuration with the ply-drops next to the thin section far from the mid-plane presents a longer fatigue lifetime.

CONCLUSIONS AND PERSPECTIVES

Two ply-drop configurations with different positions of ply-drops in thickness direction have been tested, one with the ply-drops close to the thin section close to the mid-plane (V_{int}) the other one far from the mid-plane (V_{ext}). A finite element 3D global-local model has been developed to calculate the interlaminar opening 33 and shear stress 13 around the ply-drops. By observation it has been found that delamination initiates preferably on one particular side of the specimen. Comparing the experimental observations with the numerical values shows that the side with higher frequency of delaminations has higher shear stress 13. The opening stress 33 doesn't show a clear tendency. Another observed phenomenon is that during cyclic loading for both configurations the delaminations initiate around ply-drops 1 and 2. It has been found that the numeric values of shear stress 13 are higher at ply-drop 1 and 2 than at 3 and 4, the general level of opening stress 33 is lower with no hard peaks.

Damage kinetics before final failure have been observed with a camera. After delamination propagation around ply-drop 1 and 2, the specimens divide into three sub-laminates which buckle independently. The V_{int} separates in three sub-laminates of nearly same size and finale failure occurs when one of them breaks. The V_{ext} separates in two small and one big sub-laminate, breakage of the big one leads to final failure.

The experimental results show that initial damage are delaminations at ply-drop 1 and 2 for both configurations. Contrary to what was expected, the configuration with the ply-drops next to the thin section far from the mid-plane (V_{ext}) presents a longer fatigue lifetime compared to the configuration with the ply-drops close to the mid-plane (V_{int}).

Other ply-drop configurations are under study to confirm the identified tendencies. Not only first damage and final failure but also damage kinetics will be studied more in detail. A finite element model will be developed in order to simulate delamination propagation initiated at one side in width direction.

References

1. G. B. Murri, J. R. Schaff, A. L. Dobyns, « Fatigue and damage tolerance analysis of a hybrid composite tapered flexbeam ». American Helicopter Soc. 57th Forum 2001, http://search.nasa.gov
2. D. J. Shim, « Role of delamination and interlaminar fatigue in the failure of laminates with ply dropoffs ». PhD Thesis; MIT (USA) 2002.
3. C. A. Steeves, N. A. Fleck, « Compressive strength of composite laminates with terminated internal plies ». Composites: Part A, p.1-8, 2004
4. O. T. Thomsen, F. Mortensen, Y. Frostig, « Interface failure at ply drops in CFRP/sandwich panels ». J. of Composite Materials, 34, p.135-157, 2000
5. A. Mukherjee, B. Varughese, « Design guidelines for ply drop-off in laminated composite structures ». Composites Part B, 32, p.153-164, 2001
6. R. Ganesan, D. Y. Liu, « Progressive failure and post-buckling response of tapered composite plates under uni-axial compression ». Composite Structures, 82, p.159-176, 2007